Analytical Biochemistry 675 (2023) 115212

Contents lists available at ScienceDirect

Analytical Biochemistry

journal homepage: www.elsevier.com/locate/yabio

High field brain proton magnetic resonance spectroscopy and volumetry in children with chronic, compensated liver disease – A pilot study

Cristina Cudalbu [a,b], Lijing Xin [a,b], Benedicte Marechal [c,d,e], Sarah Lachat [f], Florence Zangas-Gheri [g], Nathalie Valenza [g], Sylviane Hanquinet [h], Valérie A. McLin [f,*]

[a] CIBM Center for Biomedical Imaging, Switzerland
[b] Animal Imaging and Technology, Ecole Polytechnique Fédérale de Lausanne, Lausanne, Switzerland
[c] Advanced Clinical Imaging Technology, Siemens Healthineers International AG, Lausanne, Switzerland
[d] Department of Radiology, Lausanne University Hospital (CHUV) and University of Lausanne, Lausanne, Switzerland
[e] LTS5, École Polytechnique Fédérale de Lausanne (EPFL), Lausanne, Switzerland
[f] Swiss Pediatric Liver Center, Pediatric Gastroenterology, Hepatology and Nutrition Unit, University Hospitals Geneva, Department of Pediatrics, Gynecology and Obstetrics, University of Geneva Medical School, Geneva, Switzerland
[g] Pediatric Neurology Unit, University Hospitals Geneva, Department of Pediatrics, Gynecology and Obstetrics, University of Geneva Medical School, Geneva, Switzerland
[h] Pediatric Radiology Unit, Radiology Division, Diagnostic Department, Children's Hospital, University Hospitals of Geneva, Switzerland

ARTICLE INFO

Keywords:
Neurometabolism
Proton magnetic resonance spectroscopy
Children with chronic
Compensated liver disease
High field MRS
Glutamine

ABSTRACT

Background: There is increasing evidence that children or young adults having acquired liver disease in childhood display neurocognitive impairment which may become more apparent as they grow older. The molecular, cellular and morphological underpinnings of this clinical problem are incompletely understood.
Aim: Therefore, we used the advantages of highly-resolved proton magnetic resonance spectroscopy at ultra-high magnetic field to analyze the neurometabolic profile and brain morphometry of children with chronic, compensated liver disease, hypothesizing that with high field spectroscopy we would identify early evidence of rising brain glutamine and decreased myoinositol, such as has been described both in animals and humans with more significant liver disease.
Methods: Patients (n = 5) and age-matched controls (n = 19) underwent 7T MR scans and short echo time ^{1}H MR spectra were acquired using the semi-adiabatic SPECIAL sequence in two voxels located in gray and white matter dominated prefrontal cortex, respectively. A 3D MP2RAGE sequence was also acquired for brain volumetry and T_1 mapping. Liver disease had to have developed at least 6 months before entering the study. Subjects underwent routine blood analysis and neurocognitive testing using validated methods within 3 months of MRI and MRS.
Results: Five children aged 8–16 years with liver disease acquired in childhood were included. Baseline biological characteristics were similar among patients. There were no statistically significant differences between subjects and controls in brain metabolite levels or brain volumetry. Finally, there were minor neurocognitive fluctuations including attention deficit in one child, but none fell in the statistically significant range.
Conclusion: Children with chronic, compensated liver disease did not display an abnormal neurometabolic profile, neurocognitive abnormalities, or signal intensity changes in the globus pallidus. Despite the absence of neurometabolic changes, it is an opportunity to emphasize that it is only by developing the use of ^{1}H MRS at high field in the clinical arena that we will understand the significance and generalizability of these findings in children with CLD. Healthy children displayed neurometabolic regional differences as previously reported in adult subjects.

1. Introduction

Neurocognitive difficulties spanning attention deficit, executive functioning problems, and intellectual disability have all been described in children both before and after liver transplantation [1]. Some of these difficulties seem to evolve with patient age and time since transplant, probably owing to the increasingly complex tasks children and

* Corresponding author. Swiss Pediatric Liver Center, Department of Pediatrics, Gynecology, and Obstetrics, University of Geneva School of Medicine, Rue Willy Donzé 6, CH 1205, Geneva, Switzerland.
E-mail address: valerie.mclin@hcuge.ch (V.A. McLin).

https://doi.org/10.1016/j.ab.2023.115212
Received 10 March 2023; Received in revised form 7 June 2023; Accepted 8 June 2023
Available online 24 June 2023

adolescents are required to perform as they advance in their school curriculum. Historically, these difficulties have been ascribed to chronic illness, malnutrition, and maybe even calcineurin inhibitors use [2,3].

Abbreviations

ROI	region of interest
WM	white matter
GM	gray matter
Lac	lactate
tCr	total creatine
Tau	taurine
Ins	myoinositol
NAA	N-acetylaspartate
tCho	total choline
Glu	glutamate
Gln	glutamine
GABA	γ-aminobutyrate
Gly	glycine
GSH	glutathione
Mac	macromolecules
MP2RAGE	Magnetization Prepared 2 Rapid Acquisition Gradient Echoes
SPECIAL	spin echo full intensity acquired localized

However, mounting evidence points to measurable deficits in young infants with chronic liver disease (CLD), suggesting that the late neurocognitive challenges observed in older children may have an early onset [4,5], the underlying molecular mechanisms of which are unknown. But it has been identified that neurometabolic changes are present in adults with liver disease, and that these underlie chronic and acute encephalopathy [6,7]. It follows, therefore, that children may be subject to similar neurometabolic disturbances, which have been investigated in a few reports using magnetic resonance imaging (MRI) and proton magnetic resonance spectroscopy (^{1}H MRS) at 1.5T and 3T [8–11]. Unfortunately, while these studies have given us pointers, they have been limited by the spectral resolution of current day clinical scanners and thus the number of reliably measured metabolites. Furthermore, psychometric testing was not always available, limiting the interpretation of the MRI and MRS data [9].

Specifically, glutamine (Gln), the metabolic by-product of ammonia transformation in the brain, is difficult to distinguish from glutamate (Glu) in MR spectra at lower magnetic fields [12]. This is relevant because Gln is accepted to be the main driver in the osmotic changes in the brains of animals and humans with CLD and or hyperammonemia [13–21]. Gln elevation is classically mirrored by a decrease in myoinositol concentrations (Ins), the hallmark of the osmoregulatory response [17]. In a longitudinal animal model of chronic liver disease, Gln concentration in the brain has been shown to rise early in the course of liver disease, and to be associated at the molecular level with a decrease in Ins and with behavioral modifications [14]. Furthermore, in a model of rats having acquired CLD as pups, these changes were more pronounced suggesting that the developing brain may be uniquely vulnerable to the metabolic changes associated with CLD [15]. In addition, Ins modifications have been reported in the brains of children with chronic liver disease or portosystemic shunting [9,10]. Therefore, it follows, that to truly decipher if children with chronic, compensated liver disease harbor molecular changes in the brain that may underlie present or later neurocognitive difficulties, measuring Gln concentration reliably is essential. The ultimate goal is to determine whether early neurometabolic changes compatible with early hepatic encephalopathy are present, and ultimately elucidating whether they underlie later neurocognitive difficulties and are amenable to intervention.

In addition to the known neurometabolic changes described above, structural changes in white matter (WM) and gray matter (GM) have been described in adult subjects with cirrhosis, some of which may be reversible following liver transplantation [22,23]. What limited evidence there is in children does suggest that WM involvement may be associated with minimal hepatic encephalopathy [24], which is why we aimed to perform MRI and ^{1}H MRS in both gray and white matter, focusing on the prefrontal cortex, a key area in cognition, which has also been reported to be affected in both human and animal studies of HE [13,25–27].

Therefore, we took advantage of facilitated access to a 7T MRI scanner to investigate for the first time at such high resolution the neurometabolic profile in the brains of children with CLD and to compare them to healthy, age-matched controls. In multiple sclerosis, use of a 7T MRI scanner in children has shown very early changes previously unsuspected [28]. Hence, we hypothesized that the resolution of the 7T MRI scanner could detect early molecular changes suggestive of osmoregulatory disturbances in the brains of children with chronic liver disease at very early stages.

2. Material and methods

2.1. Subjects

For this pilot and observational study, patients were recruited through clinic visits. Inclusion criteria were the following: children with compensated chronic liver disease (CLD >6 months) aged between 8 and 16 years. Patients with any congenital, genetic, or acquired liver disease of childhood were eligible. Disease-specific exclusion criteria included decompensated CLD, use of antibiotic or psychoactive substances interfering with neurometabolism <4 weeks prior to testing, general anaesthesia within 72 h. The following laboratory studies were obtained as part of routine clinical care within 1 month of the MRI/MRS and neurocognitive assessment: full blood count, liver panel, coagulation panel, and fasting plasma ammonia. In addition, patient records were queried for historical values, specifically maximum plasma bilirubin concentration during follow-up. An evaluation of hepatic fibrosis was made by ultrasound elastography with the Acoustic Radiation Force Impulse ARFI (VTQ) module (Acuson® S3000 imaging, Siemens, Germany); ARFI measures the speed of a shear wave in the examined tissue in meters per second (m/s).

Controls (CTR) were recruited by word of mouth and among family members of patients to obtain age-matched subjects. Additional controls were also recruited through public advertisement at the hospital and Faculty of Medicine. Controls underwent a screening interview for basic medical history and a clinical exam.

All subjects were scrutinized for method-specific exclusion criteria including dental braces, cardiac device, metal prosthesis, etc. or any other contraindication to MRI like claustrophobia and pregnancy. All subjects were enrolled following written and informed consent. The study was approved by the institutional review board (CCER 2017-01854).

2.2. ^{1}H MRS/MRI and image processing

^{1}H MRS/MRI data were acquired on an investigational 7T/68 cm MRI scanner (MAGNETOM 7T, Siemens Healthcare, Erlangen, Germany) using a single-channel quadrature transmit and 32-channel receive coil (Nova Medical Inc., MA, USA).

A 3D MP2RAGE sequence [29](TR = 6 s, TE = 2.05 ms, TI1 = 0.8 s, TI2 = 2.7s, α1 = 4°, α2 = 5°, 0.6 × 0.6 × 0.6 mm^3 resolution, 320 × 320 × 256 matrix size, TA = 10min) was used to: i) collect high resolution images for MRS voxel positioning; and ii) generate T_1 maps for investigating the T_1 relaxation times in the globus pallidus in particular. Since brain atrophy was recently reported in adults with CLD, automated

segmentation of deep brain structures was performed using the MorphoBox prototype [30,31]. Absolute volume and average T_1 values were calculated over each basal ganglia nuclei segmentation mask (caudate, putamen, thalamus, pallidum), hippocampus and amygdala obtained by non-rigidly registering an age-appropriate atlas [32] developed at 1.5T representing the average age range anatomy for 8–16 years to the MP2RAGE uniform input image and propagating the six different anatomical labels. In addition, signal intensity variability of the GP (Globus pallidum) and the adjacent putamen was quantified using measurements of the average intensity on the 3D MP2RAGE sequence (UNI image, axial reconstruction), utilizing a manual elliptical (20 mm^3) region-of-interest (ROI) with the OsiriX brush tool (SH, senior pediatric radiologist, OsiriX MD v 12.5.2 software (Geneva, Switzerland). The mean of the measurements in the right and left region was reported for each patient. ROI values ratio (Putamen/GP) were calculated for both CLD children and the control group [9]. Each ROI was placed manually to quantify the signal from the same area for all subjects for the purposes of ratio calculation (Putamen/GP) as previously described [9], where differences in signal intensity and Putamen/GP ratios have been detected between children with chronic liver disease or porto-systemic shunting and controls.

^{1}H MRS was performed using the semi-adiabatic SPECIAL sequence at short echo-time (16 ms) in two voxels (Supplementary Material 1 and 2) positioned in gray matter (GM) dominated (20 × 20 × 25mm^3) and white matter (WM) dominated (15 × 16 × 18mm^3) prefrontal cortex (TR = 6500 ms, 2 × 50 averages (i.e. acquisitions per spectrum), spectral width of 4000 Hz, 2048 points in FID) [33,34]. Metabolite quantification was performed using LCModel [35] (Supplementary Material 3) combined with a simulated basis set using published values of J-coupling constants, chemical shifts [36,37], including an in vivo acquired macromolecules spectrum, and ratios to tCr since the water content and metabolite T_2 relaxation times are not yet known for the age range investigated in the present study at 7T. The following metabolites were included in LCModel basis set: alanine (Ala), ascorbate (Asc), aspartate (Asp), glycerophosphocholine (GPC), phosphocholine (PCho), creatine (Cr), phosphocreatine (PCr), γ-aminobutyric acid (GABA), glutamine (Gln), glutamate (Glu), glutathione (GSH), glycine (Gly), inositol (Ins), lactate (Lac), N-acetylaspartate (NAA), N-acetylaspartylglutamate (NAAG), phosphoethanolamine (PE), taurine (Tau), glucose (Glc), scyllo-inositol (Scyllo) and serine (Ser). PCho and GPC were expressed only as tCho (PCho + GPC) due to better accuracy in the estimation of their concentration as a sum. Supplementary Material 4 summarizes the minimum reporting standards in MRS [38]. As the in vivo acquired macromolecules spectrum was added to the metabolite basis set and no lipid contamination was noticed in the acquired spectra, the lipids as provided by LCModel were omitted from the fit.

2.3. Cognitive testing

Patients underwent a neurological assessment Unified Wilson's Disease Rating Scale (UWDRS) (30 min) and a series of validated, age-appropriate neurocognitive tests to explore global cognitive functioning and attention span, using the tests Wechsler Intelligent Scale for Children (WISC-IV) and Conners Continuous Performance Task (CPT-2 or CPT-3). Details regarding these tests are available in Supplementary materials (Supplementary Material 5).

2.4. Statistical analyses

^{1}H MRS and MRI: Results are presented as mean ± standard deviation (SD). Two-way ANOVA (Prism 5.03, Graphpad, La Jolla CA USA) with respect to each metabolite in the neurochemical profile or MRI parameter followed by Bonferroni's multiple comparisons post-test was used when comparing the two groups (CTR vs CLD) in the two brain regions (GM vs WM) (group or brain region as repeated factor, 2 comparisons) and the controls (CTR) at different ages (8–10, 11–12, 13–14 and 15–16 years) in the two brain regions (GM vs WM) (age as repeated factor, 4 comparisons). In addition, one-way ANOVA was used when evaluating the T_1 relaxation times and brain volume differences with age for CTRs per each brain region individually (age as repeated factor, 6 comparisons); for the brain regional difference in T_1 relaxation times for the averaged CTR group (brain regions as repeated factor, 15 comparisons); and for the brain metabolites evolution for the age range of 8–10 years for both groups (CTR vs CLD) (brain regions and groups as repeated factor, 6 comparisons). All tests were 2-tailed. Significance in all tests was attributed according to: *$p < 0.05$; **$p < 0.01$; ***$p < 0.001$; ****$p < 0.0001$.

3. Results

3.1. Subject characteristics

Five patients (5; 2 girls) and nineteen (19; 10 girls) controls underwent MRI and ^{1}H MRS at 7T between January 2018 and August 2019.

Table 1
Patient and control characteristics.

			Gender				
PATIENTS	Diagnosis	n	m	f	Age	Z-Score weight	Z-Score height
	PFIC 2	1	1		14.5	−1.08	−1.18
	AIH	1	1		9	0.04	−0.52
	CDG1b	1		1	8	−1.13	−2.3
	Portal cavernoma	1		1	12	0.28	0.2
	Biliary atresia	1	1		8	1.8	3.07
	total	**5**	**3**	**2**		* https://www.quesgen.com/BMIPedsCalc.php	

CONTROLS		n	m	f	Mean age	Mean Z-Score weight	Mean Z-Score height
Age groups	8–10	4	1	3	8.6	0.12	0.54
	11–12	5	3	2	10.5	0.40	0.62
	13–14	6	2	4	12.8	0.35	0.87
	15–16	3	2	1	14.3	−0.08	0.38
	total	**18**	**8**	**10**		https://www.quesgen.com/BMIPedsCalc.php	

Table 2
Patient and control characteristics. ^{1}H MRS: proton magnetic resonance spectroscopy, Dx: diagnosis, Bili max: maximum bilirubin concentration, Tc: thrombocytes, ALT: alanine aminotransferase, ARFI: acoustic radio force impedance, WISC: Wechsler Intelligence Scale for Children, CPT: Continuous Performance Test, CDG1b: congenital disorder of glycosylation, PFIC: progressive familial intrahepatic cholestasis, AIH: autoimmune hepatitis. WISC and CPT scores are expressed relative to a normative population. #: number of parameters below the norm. Values in red are out of the normal range.

Diagnosis	Age 1H-MRS (years)	Age 1H-MRS (months)	Age Dx (years)	Age Dx (months)	Bili max total (μmol/l)	*Age specific ref range*	Bili at MRS (μmol/l)	*Age specific ref range*	Tc (G/L) *NL 200-400*	ALT (U/L) *seuil 0-18*	NH_4^+ (μmol/L) *NL 11-35*	ARFI m/sec	WISC QIT	CPT #
PFIC	14 + 7 months	175	0	2	18	*7-25*	14	*7-25*	346	45	24	1.5	1.27	0
Type 1 AIH	9 + 3 months	111	7	84	22	*0-5*	11	*0-8*	219	24	40	1.09	3.06	3
CDG Ib	8 + 8 months	104	7	82	7	*0-8*	4	*0-8*	79	28	33	1	-1.4	0
Portal cavernoma	12 + 2 months	146	12	143	11	*0-10*	6	*0-10*	59	27	12	1.3	-0.73	0
Biliary atresia	8 + 3 month	99	0	3	240	*7 - 25*	3	*0-5*	325	31	39	1.4	2.1	0

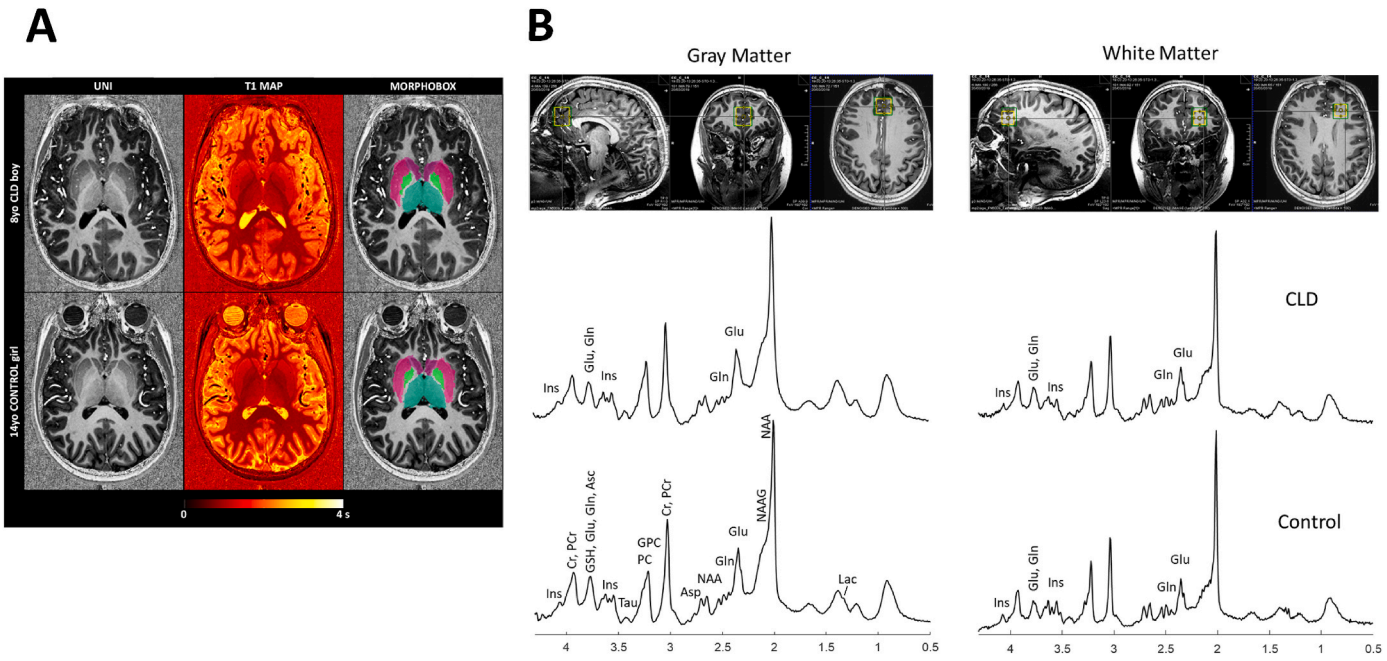

Fig. 1. A: Representative axial slices MP2RAGE uniform contrast (left), T_1 maps (middle) and corresponding basal ganglia nuclei segmentation masks (right) of a 8 year-old CLD boy (top) and a 14 year old female CTR (bottom). **B:** Representative ^{1}H MRS spectra with corresponding voxel position and size on anatomical images (green voxel for shimming, yellow voxel for ^{1}H MRS) acquired at 7T in two different voxels located in GM (20 × 20 × 25mm^3) and WM (15 × 16 × 18mm^3) dominated prefrontal cortex in CLD and CTR. Acquisition parameters: semi-adiabatic SPECIAL sequence, TE = 16 ms, TR = 6500 ms, 2 × 50 averages, spectral width of 4000 Hz, 2048 points in FID. No post-processing was applied except for B0 drift and eddy current corrections. The main metabolites are labelled on the spectrum acquired in the GM CTR while for the other spectra only the main metabolites involved in CLD induced-HE are labelled. GM: gray matter dominant, WM: white matter dominant.

Patient and control characteristics are summarized in Table 1. Age groups were defined by birthdays (tenth birthday = end of the tenth year of life; beyond that the child enters his/her eleventh year and is considered in the 11–12 age group). While the ages were similar between subjects and controls, the CLD group displayed a wider range of height and weight Z-scores compared to the control group. Time spent in the scanner varied between 45 min and 75 min. Controls subjects were divided into the following age groups: 8–10, 11–12, 13–14 and 15–16 (Table 1). Patient characteristics are further detailed in Table 2. Diagnoses were representative of a pediatric liver disease practice. All enrolled patients were feeling well and attending school normally.

3.2. MRI results

High quality 3D T_1-weighted MP2RAGE images were obtained for all patients (n = 5 for CLD) and 18 controls (n = 18 for CTR) as one control child was excluded due to movement (Fig. 1A and Supplementary Material 6). No morphological brain abnormality was observed on the single sequence in either patients or controls.

Given the unprecedented nature of the study, and lack of normative data, we used the data from the 18 healthy volunteers to evaluate possible changes in basal ganglia nuclei, amygdala, hippocampus brain volumes and T_1 relaxation times among the different age groups (8–10, 11–12, 13–14, 15–16 years; Fig. 2 A and B). No statistically significant age-related differences were observed in the brain volumes or overall T_1

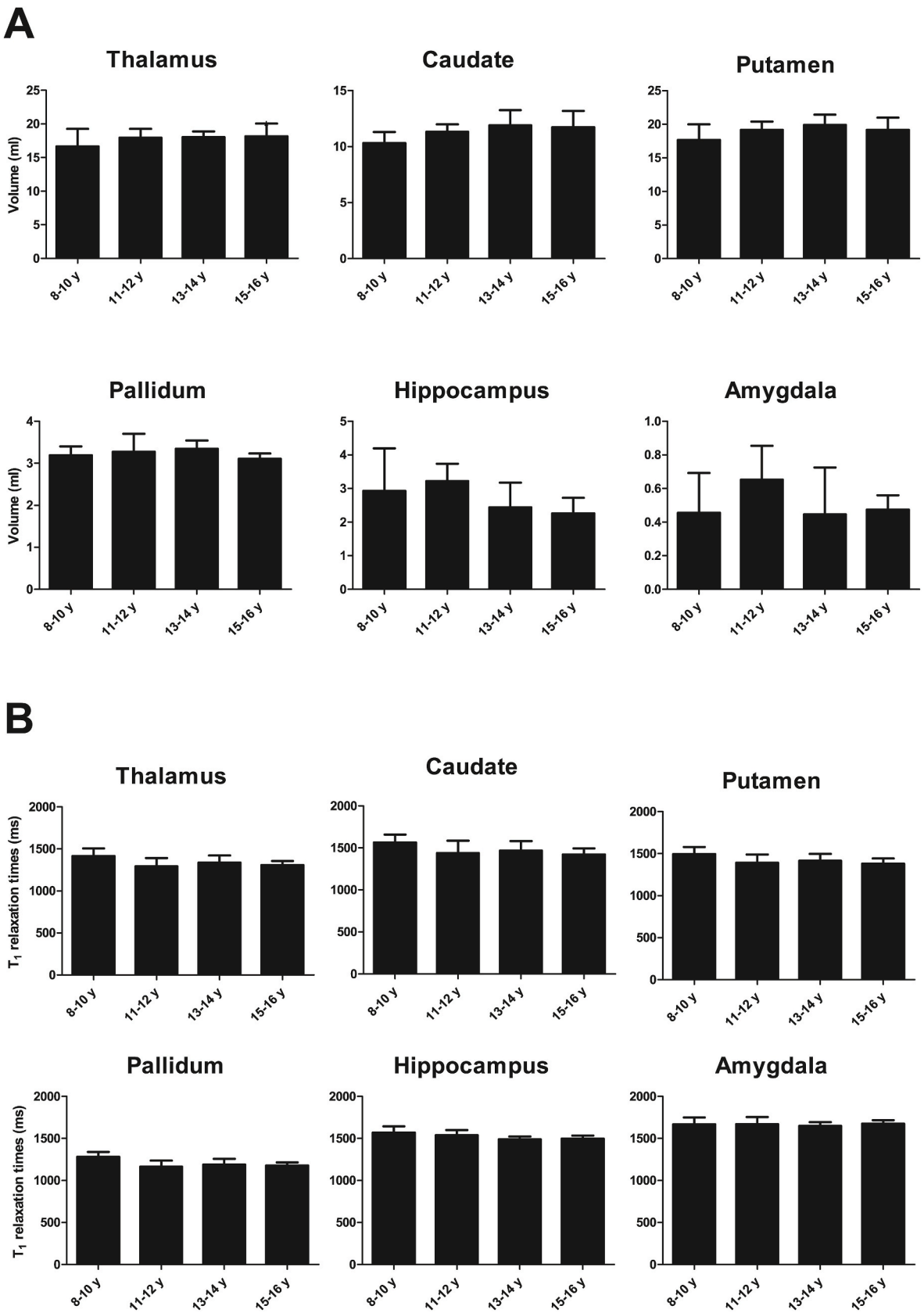

Fig. 2. Absolute brain volumes in milliliters (ml) (**A**) and T_1 relaxation times in milliseconds (ms) (**B**) volume according to age in control volunteers in six different brain regions (n = 18 volunteers in total with n = 4 (8–10 years), n = 5 (11–12 years), n = 6 (13–14 years), n = 3 (15–16 years)). No statistically significant age-related differences were observed. Data are presented as Mean ± SD.

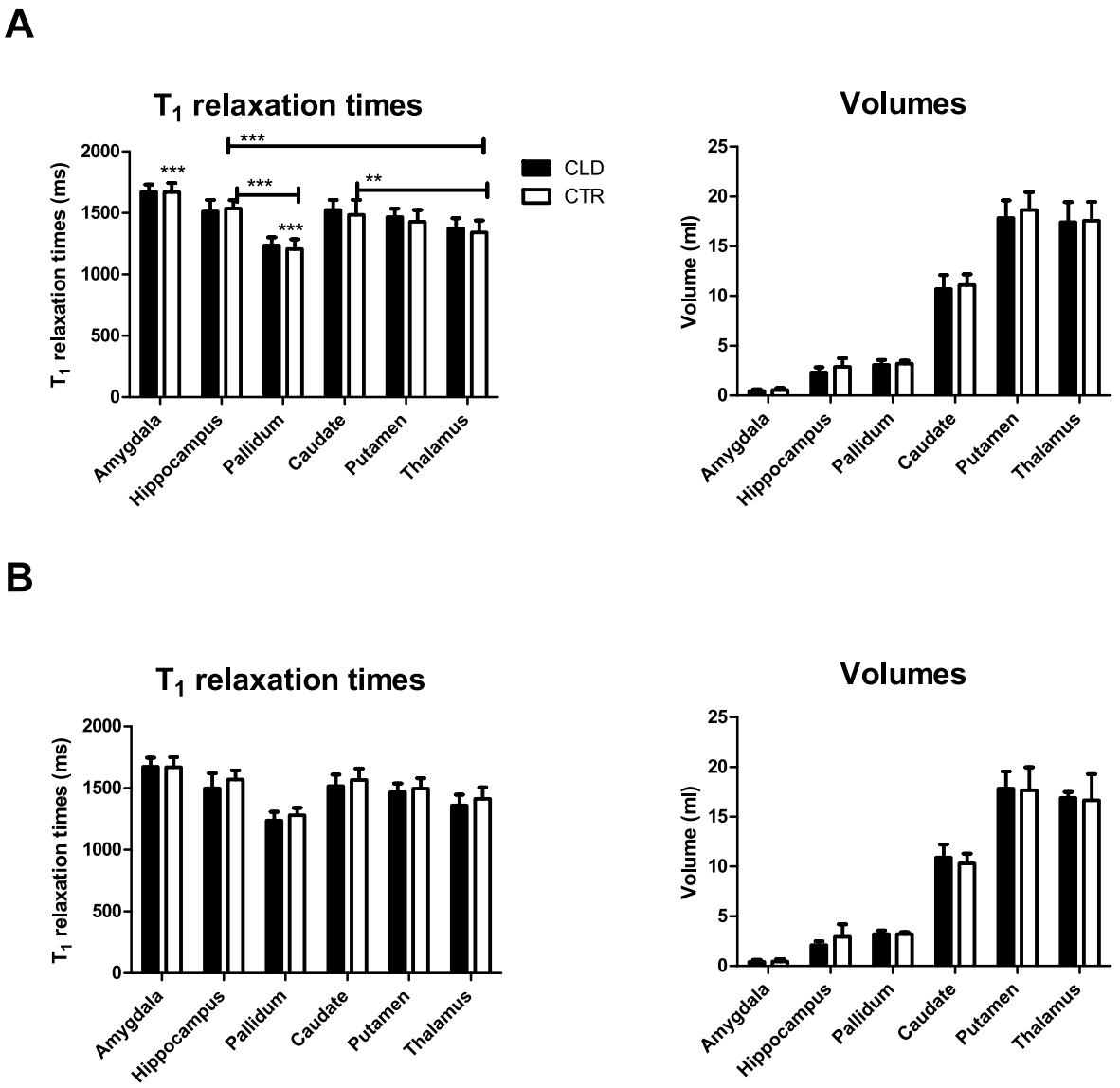

Fig. 3. Absolute brain volumes (ml) and T_1 relaxation times (ms) evolution between CLD (black bars) and CTR (white bars) in six different brain regions. **A**) Averaged values over all CLD patients (n = 5) and all CTR volunteers except the age range of 13–14 years (n = 12). **B**) Averaged values only for the 8–10 years bracket for both CLD (n = 3) and CTR (n = 4). There was a statistically significant difference in T_1 relaxation times between the amygdala and pallidum and all other regions (***).

Data are presented as Mean ± SD. Significance in the one-way ANOVA tests was attributed according to: *p < 0.05; **p < 0.01; ***p < 0.001; ****p < 0.0001.

Table 3
Deep nuclei signals GP globus pallidus, Put putamen *: no patients in the 13–14 age bracket.

Age (Years)	Mean ± SD Put	Median Put	Mean ± SD GP	Median GP	Mean ± SD Ratio Put/GP	Median Ratio Put/GP
8–10 N = 4	1155.5 ± 314.5	1045	2025.7 ± 348.2	1867	1.8 ± 0.2	1.8
11–12 N = 5	1533.2 ± 342.5	1448	2383.8 ± 285.9	2385	1.6 ± 0.2	1.7
13–14 N = 6	1415.6 ± 261.2	1308	2238.2 ± 283.9	2142	1.6 ± 0.1	1.6
15 - 16 n = 3	1422. 0 ± 155.6	1417	2270.0 ± 125.4	2239	1.6 ± 0.1	1.6
Patients 8–16 n = 5*	1270.4 ± 207.4	1324	2096.2 ± 255.0	2134	1.7 ± 0.1	1.6

relaxation time of CTR. However, a significant regional difference was observed in the T_1 relaxation times (T_1s) according to brain region: lowest T_1s for pallidum and highest T_1s for amygdala) (Fig.. 2 B and 3 A).

The estimated brain volumes and T_1 relaxation times averaged over the entire CLD group were compared to those averaged in the CTR group (Fig. 3A) for the six brain regions. In this analysis, the 13–14 years age group was excluded from the CTR group since there was no CLD subject in the corresponding age range. The CLD group had three patients with the age range of 8–10 years, therefore the MRI and MRS data from these patients were compared to the corresponding CTR group (n = 4)

(Fig. 3B). No statistically significant differences were observed between CLD and CTR for any of the comparisons.

Given that MRI signal intensity of the Globus pallidus (GP) is accepted to be a hallmark of hepatic encephalopathy, a quantitative measurement was performed in all children (one exclusion owing to movement artefact). The GP signal was visually identical in the whole cohort. The ROI values and Putamen/GP ratios were not significantly different between CLD and CTR (Table 3).

3.3. ^{1}H MRS results

GM spectra were acquired in all 5 CLD patients and 14/19 CTR children. Four spectra were not acquired due to movement and one owing to patient refusal. In the CLD group, four WM spectra were

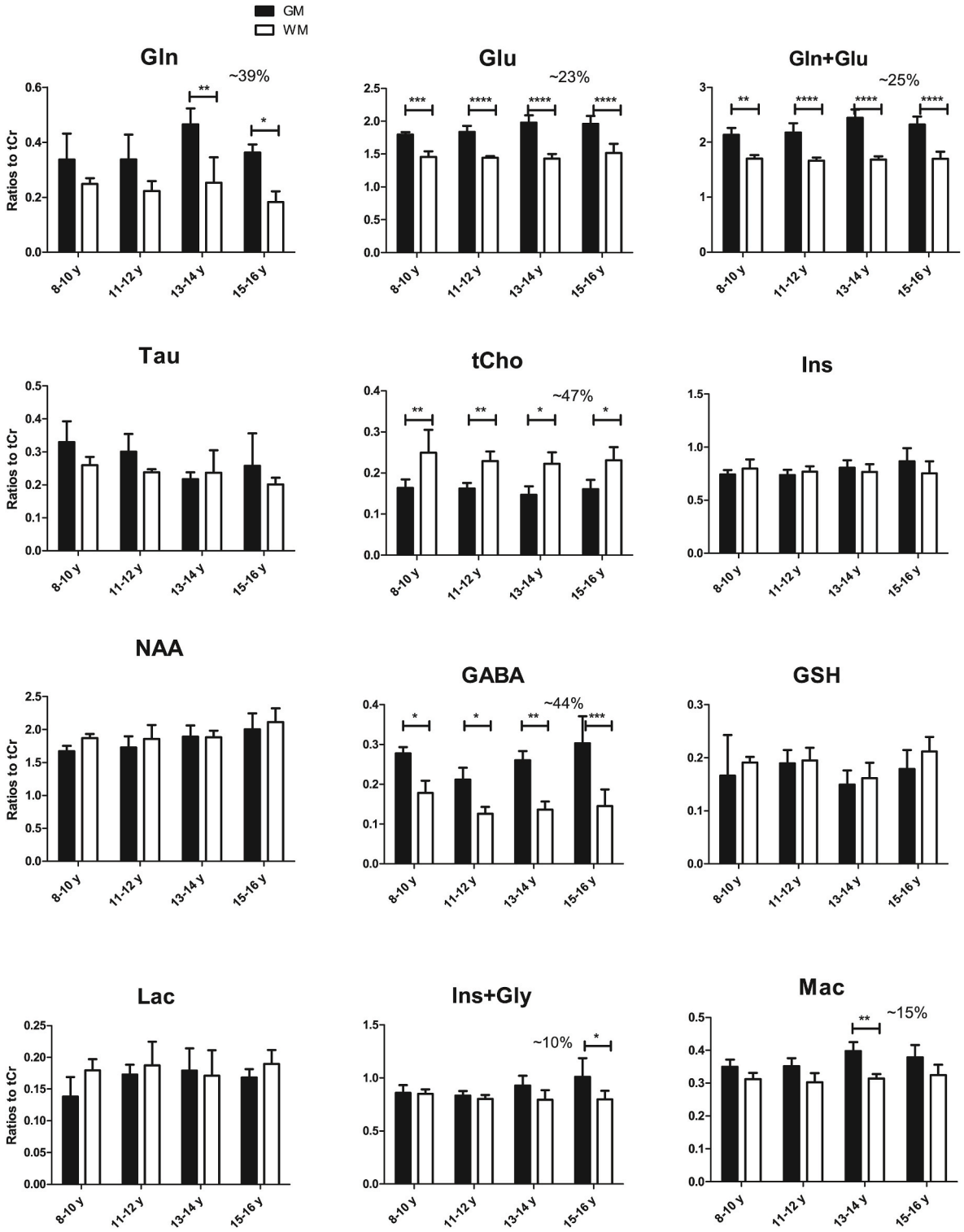

Fig. 4. Brain metabolites evolution with age in CTR in GM and WM dominated voxels positioned in prefrontal cortex. Black bars represent the metabolite ratios to tCr in GM, while white bars the metabolite ratios to tCr in WM. The percentage changes shown in the figure represent the mean change between GM and WM. Data are presented as Mean ± SD. Significance in the two-way ANOVA tests was attributed according to: *p < 0.05; **p < 0.01; ***p < 0.001; ****p < 0.0001.

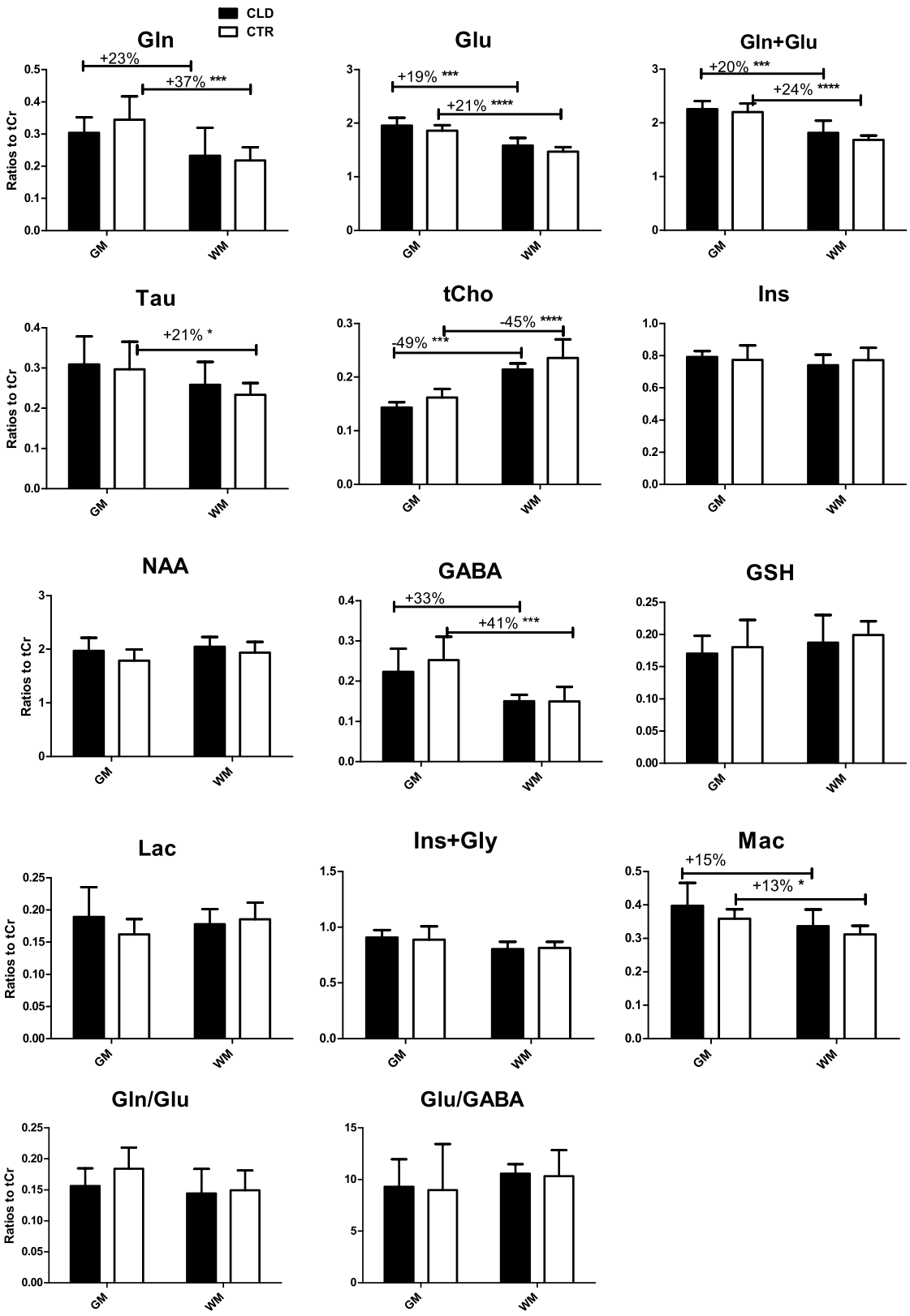

Fig. 5. Brain metabolite changes between CLD and CTR groups in GM and WM dominated voxels positioned in prefrontal cortex. Black bars represent the metabolite ratios to tCr in GM, while white bars the metabolite ratios to tCr in WM. The percentage changes shown in the figure represent the change between GM and WM. Data are presented as Mean ± SD. Significance in the two-way ANOVA tests was attributed according to: *$p < 0.05$; **$p < 0.01$; ***$p < 0.001$; ****$p < 0.0001$.

acquired, with one patient refusing to finish the study. In the CTR group 13 WM spectra were acquired: 4 spectra not acquired due to increased movement, 2 owing to patient requesting early termination of the study (Supplementary Material 6).

Examples of spectra obtained in the WM and GM of controls and patients are illustrated in Fig. 1B. High quality spectra were acquired with a mean signal-to-noise ratio of 62.9 ± 6.6 in GM and 56.5 ± 7.3 in WM, and a mean linewidth of 0.033 ± 0.009 ppm (9.8 ± 2.6 Hz) in GM and 0.031 ± 0.007 ppm (9.2 ± 2.1 Hz) in WM as provided by LCModel quantification. Furthermore, the water linewidths ranged between 9 and 12 Hz in agreement with the values provided in the B_0 shimming consensus recommendations [39]. First, we plotted brain metabolite changes in GM and WM of controls and among the different age groups with the aim to identify whether developmental changes are occurring between the ages of 8–16 years. The only appreciable change was a trend toward decreased Tau (~20%) and increased NAA (~15%) which did not reach significance (Fig. 4). Significant differences in metabolite ratios to tCr were however observed between GM and WM for the following metabolites: Gln (~39%), Glu (~23%), tCho (~47%), GABA (~44%) and Mac (~15%). For the sum of Ins + Gly this difference was mainly for the 15–16 years (~10%). All these brain regional differences were consistent across the four age groups.

The metabolite ratios to tCr estimated for the entire CLD group were compared to those averaged over the entire CTR group in the age range (8–10, 11–12, 15–16 years, Fig. 5) for both brain regions. The age group of 13–14 years was excluded from the CTR group since there was no CLD child in this age group. As can be seen no significant changes between CLD and CTR children were measured. However, like for the CTR group (Fig. 4), a brain regional difference was measured for the CLD group, and the changes in the specific metabolites (Gln, Glu, tCho, GABA, Mac) were similar to those observed in CTR. In addition, a brain regional change in Tau was observed (~21%) reaching significance only for WM in the CTR group.

As for the MRI data, the metabolite ratios to tCr from the age range of 8–10 years were compared between CLD and CTR groups in the two brain regions (Fig. 6). A statistically insignificant increase of Glu and NAA was observed in both brain regions in children with CLD. As for the previous comparisons, the brain regional difference was also confirmed in these two groups (e.g. Glu, Tau, tCho, GABA, Mac).

3.4. Cognitive testing

All patients with CLD showed scores in range or above average on Total Intellectual Quotient measured with the WISC-IV and had homogenous profiles on this scale. Only one patient, who was migrant and was not fluent in the testing language, showed an IQ score close to the lower limit. Only one patient scored below average on several parameters on the Conners Continuous Performance Test, suggesting attention deficit. The other CLD patients placed within the normal range.

4. Discussion and conclusion

In a highly selected group of children aged 8–16 years with compensated, chronic liver disease, there was no evidence of Gln increase or osmoregulatory imbalance compared to age-matched controls using ^{1}H MRS at 7T in both white-matter dominant and gray-matter dominant areas of the prefrontal cortex in spite of documented, mild hyperammonemia in 2 subjects at the time of the study, and in all 5 patients at some point during their follow up. In addition, brain volume and regional volume analyses showed no differences between CLD and CTR, unlike previous reports in adult patients that HE may be associated with lower brain volumes [13,40] and that lower brain volume have been reported in children with CLD [41]. In the limited sample size of this pilot study, we observed a slight increase of Glu and NAA in children with CLD in both brain regions something previously unreported in children with CLD [24]. However, the difference with healthy subjects did not reach statistical significance, and the clinical significance is unclear. Indeed, no major neurocognitive deficits were observed, but one patient did display evidence of attention deficit disorder, a common condition in the general population. Although this is the first study exploiting the advantages of ultra-high field ^{1}H MRS and MRI to analyze the neurometabolic profile and morphometry of children with chronic, compensated liver disease, the findings need to be interpreted with caution owing to the sample size limitation. That said, it is an opportunity to emphasize that it is only by developing the use of ^{1}H MRS at high field in the clinical arena that we will understand the significance and generalizability of these findings in children with CLD. Furthermore, the present studies are of broader implication for the use of MR in pediatric neurology.

Despite the absence of a Gln increase in both the WM- and GM-dominant brain regions of children with CLD, our study exhibits the feasibility of detecting Gln and Glu separately, a methodology of the utmost relevance for analyzing the molecular underpinnings of the neurocognitive manifestations of CLD. Gln has been shown to be the main driver in the osmotic changes related to liver disease and portosystemic bypass both in animal models and humans with CLD [13–20]. Furthermore, in a rat model of juvenile onset CLD, Gln increase is more pronounced than in the brains of rats having acquired CLD as adults, suggesting that the developing brain may be uniquely vulnerable to the metabolic insults associated with CLD [15]. Therefore, it is our assessment that the resolution offered by high-field magnets should continue to be exploited - and the expertise developed-in the clinical management of children and adults with CLD both for diagnostic purposes and to follow the potential impact of treatment, as has been shown in the rat model [19,20].

A regional difference was observed for Gln, Glu, Tau, GABA, macromolecules and tCho in both CTR and CLD kids at all ages. The higher GABA/tCr ratios in cortical GM compared to WM are in agreement with previous MRS and MRSI reports [42]. From a biochemical point of view, the higher GABA/tCr in GM could reflect the GABAergic synapses that are predominantly located in the GM. Further, GABA is mainly metabolized from Glu via glutamate decarboxylase, and Glu is known to exhibit a GM/WM contrast, something confirmed in the present study [42]. The higher Gln/tCr, Glu/tCr, Glx/tCr in GM and higher tCho/tCr in WM are also in agreement with previous results [43,44]. Regarding the regional differences in macromolecules, we estimated a higher macromolecules contribution in GM than in WM (ranging from 11% to 15% depending on the group; estimated using one single spectrum for the full macromolecule contribution in the metabolite basis set) which is also in agreement with previous studies [45].

We also reported the T_1 relaxation times in CLD and CTR groups in six brain regions, with no statistical difference between CTR and CLD groups. The reported values are in agreement with previously published T_1 relaxation times measured in healthy adults at 7T [29]. Hepatic encephalopathy is characterized by shortening of relaxation times in basal ganglia causing hyperintensities on T_1w images, which were not detected in this study, suggesting that HE was mild or absent in these subjects, something which fits with the minimal neurometabolic changes. That said, it is generally believed that HE associated with chronic liver disease in children, even compensated, is very different from chronic HE in adults, because it occurs in the setting of intense neurodevelopment [46] and is associated with long-term sequelae [4,5,47].

While this is the first study benefiting from the advantages of a high magnetic field to examine the brains of pediatric patients suffering from CLD, it does present several limitations. First, the sample size was small in each age group (n = 3 to 5 per group) while the overall number of children with CLD was small. Next, we were not able to verify that the patients had the typical hyperintensity in the globus pallidus as previously described in chronic hepatic encephalopathy [9,48]. While this is surprising, it may be due to patient selection and sample size. These unexpected findings may also reflect patient participation bias, namely

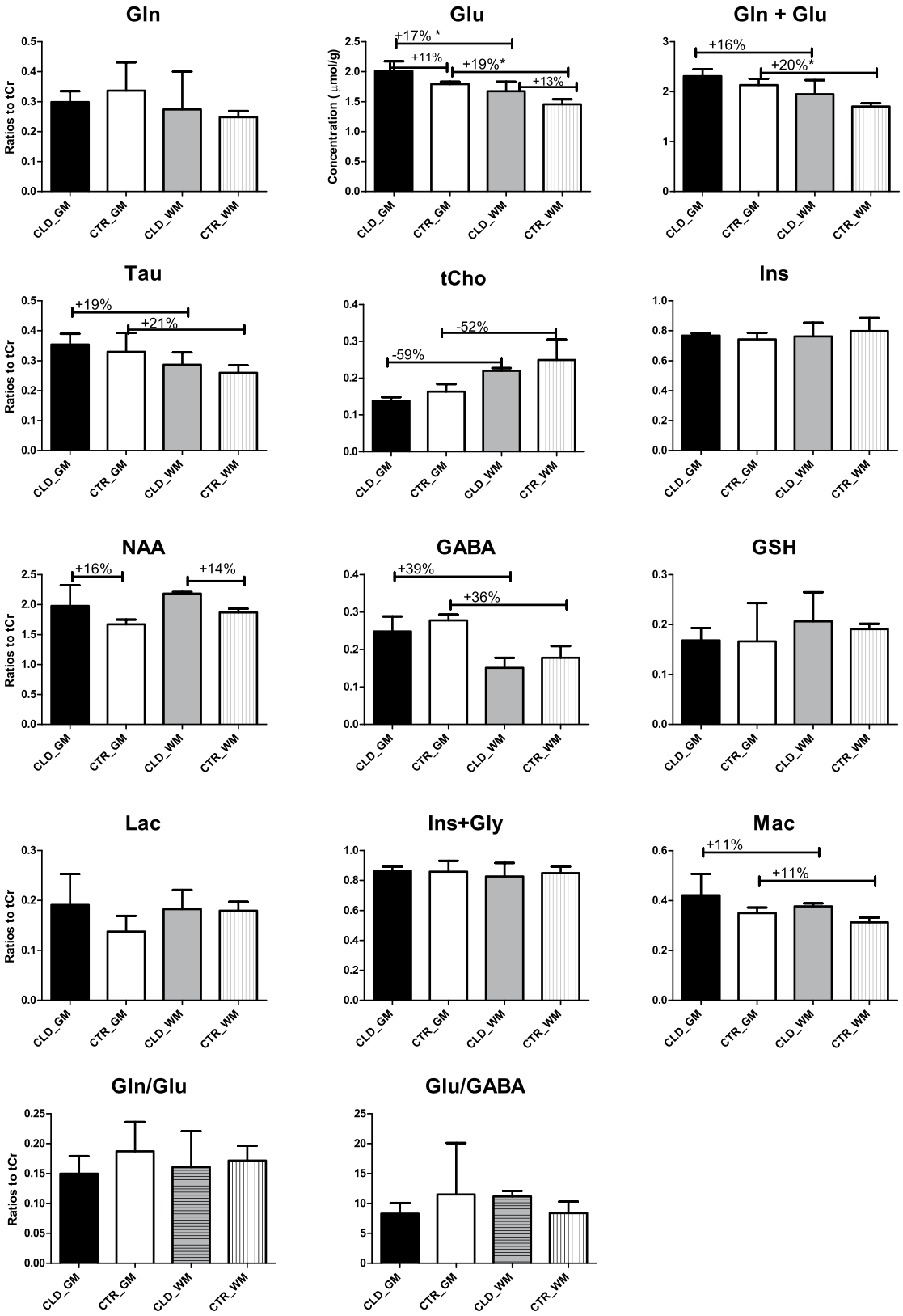

Fig. 6. Brain metabolite changes between CLD and CTR groups in the GM and WM of the 8–10 years age group. Voxels were positioned in the prefrontal cortex. The percentage changes shown in the figure represent the change between CLD and CTR, or GM and WM. GM: gray matter dominant, WM: white matter dominant. Data are presented as Mean ± SD. Significance in the one-way ANOVA tests was attributed according to: *$p < 0.05$; **$p < 0.01$; ***$p < 0.001$; ****$p < 0.0001$.

that patients who were doing well were more likely to participate than patients who declined. Finally, another limitation of the study which warrants further exploration is the gender factor [4]: while boys and girls were equally represented in the control group, there were too few per age group to reach any meaningful conclusions.

Importantly, this study adds to the body of literature documenting the use of high field studies in children [49]. In addition, it reports brain volumes and T_1 relaxation times using MRI and ^{1}H MRS findings in two brain regions in a group of healthy children aged between 8 and 16 years. We observed that the long acquisition times required to position the two MRS voxels, shim and calibrate the MRS sequence in two brain regions were difficult to sustain for children, especially those unaccustomed to the constraints of medical procedures. Therefore, automatic procedures will be a significant asset for the use of 7T in the clinical setting, especially for their use in children [50]. Moreover, the use of fast MR spectroscopic imaging techniques would allow the concomitant acquisition of several voxels in a 2D slice in the brain or even a 3D volume enabling the measurement of several metabolic maps [51,52]. Building upon currently used algorithms and experience should put this goal within easy reach [28,53,54].

Author contributions

Conceptualization, CC and VM; Methodology, CC, LX, SH; Software BM, CC, SH, LX; Validation, CC, LX; Formal Analysis, CC, VM, BM, LX; Investigation, CC, LX; Data Curation, SL; Writing – Original Draft Preparation, CC, VM, FZ, SH; Writing – Review & Editing, CC, VM, FZ, SH; Supervision, CC and VM; Project Administration, CC, SL, VM; Funding Acquisition, CC and VM.

Declaration of competing interest

The authors declare that they have no known competing financial interests or personal relationships that could have appeared to influence the work reported in this paper.

Data availability

Data will be made available on request.

Acknowledgements and funding information

This works was supported by the Swiss National Science Foundation award n° 310030_173222 and 310030_201218 and by the Center for Biomedical Imaging of the UNIL, UNIGE, HUG, CHUV, EPFL, the Leenaards and Jeantet Foundations. The authors thank the administrative and nursing staff who participated in patient recruitment and management. We are indebted to the enthusiastic volunteers for their time and interest. Special thanks go to Andrea Gropman for helpful discussions and to Sandra da Costa for to ensure participant comfort in the magnet. We thank Tobias Kober from Siemens Healthineers for use of the MP2RAGE WIP 944 and for his thoughtful review of the manuscript and to Brayan Alves for his help with some figures.

Appendix A. Supplementary data

Supplementary data to this article can be found online at https://doi.org/10.1016/j.ab.2023.115212.

References

[1] L.G. Sorensen, K. Neighbors, K. Martz, F. Zelko, J.C. Bucuvalas, E.M. Alonso, G. Studies of Pediatric Liver Transplantation Research, G. the Functional Outcomes, Longitudinal study of cognitive and academic outcomes after pediatric liver transplantation, J. Pediatr. 165 (2014) 65–72, e62.
[2] S.M. Stewart, C. Hiltebeitel, J. Nici, D.A. Waller, R. Uauy, W.S. Andrews, Neuropsychological outcome of pediatric liver transplantation, Pediatrics 87 (1991) 367–376.
[3] S.M. Stewart, C.H. Silver, J. Nici, D. Waller, R. Campbell, R. Uauy, W.S. Andrews, Neuropsychological function in young children who have undergone liver transplantation, J. Pediatr. Psychol. 16 (1991) 569–583.
[4] S.E. Caudle, J.M. Katzenstein, S. Karpen, V. McLin, Developmental assessment of infants with biliary atresia: differences between boys and girls, J. Pediatr. Gastroenterol. Nutr. 55 (2012) 384–389.
[5] S.E. Caudle, J.M. Katzenstein, S.J. Karpen, V.A. McLin, Language and motor skills are impaired in infants with biliary atresia before transplantation, J. Pediatr. 156 (2010) 936–940 e931.
[6] P. Monfort, O. Cauli, C. Montoliu, R. Rodrigo, M. Llansola, B. Piedrafita, N. El Mlili, J. Boix, A. Agusti, V. Felipo, Mechanisms of cognitive alterations in hyperammonemia and hepatic encephalopathy: therapeutical implications, Neurochem. Int. 55 (2009) 106–112.
[7] V.P. Grover, J.M. Tognarelli, N. Massie, M.M. Crossey, N.A. Cook, S.D. Taylor-Robinson, The why and wherefore of hepatic encephalopathy, Int. J. Gen. Med. 8 (2015) 381–390.
[8] S.K. Yadav, A. Srivastava, A. Srivastava, M.A. Thomas, J. Agarwal, C.M. Pandey, R. Lal, S.K. Yachha, V.A. Saraswat, R.K. Gupta, Encephalopathy assessment in children with extra-hepatic portal vein obstruction with MR, psychometry and critical flicker frequency, J. Hepatol. 52 (2010) 348–354.
[9] S. Hanquinet, C. Morice, D.S. Courvoisier, V. Cousin, M. Anooshiravani, L. Merlini, V.A. McLin, Globus pallidus MR signal abnormalities in children with chronic liver disease and/or porto-systemic shunting, Eur. Radiol. 27 (2017) 4064–4071.
[10] B.R. Foerster, L.S. Conklin, M. Petrou, P.B. Barker, K.B. Schwarz, Minimal hepatic encephalopathy in children: evaluation with proton MR spectroscopy, AJNR Am. J. Neuroradiol. 30 (2009) 1610–1613.
[11] A.A. Razek, A. Abdalla, A. Ezzat, A. Megahed, T. Barakat, Minimal hepatic encephalopathy in children with liver cirrhosis: diffusion-weighted MR imaging and proton MR spectroscopy of the brain, Neuroradiology 56 (2014) 885–891.
[12] R. Gruetter, S.A. Weisdorf, V. Rajanayagan, M. Terpstra, H. Merkle, C.L. Truwit, M. Garwood, S.L. Nyberg, K. Ugurbil, Resolution improvements in in vivo 1H NMR spectra with increased magnetic field strength, J. Magn. Reson. 135 (1998) 260–264.
[13] C. Cudalbu, S.D. Taylor-Robinson, Brain edema in chronic hepatic encephalopathy, J. Clin. Exp. Hepatol. 9 (2019) 362–382.
[14] O. Braissant, V. Rackayova, K. Pierzchala, J. Grosse, V.A. McLin, C. Cudalbu, Longitudinal neurometabolic changes in the hippocampus of a rat model of chronic hepatic encephalopathy, J. Hepatol. 71 (2019) 505–515.
[15] V. Rackayova, O. Braissant, A.L. Rougemont, C. Cudalbu, V.A. McLin, Longitudinal osmotic and neurometabolic changes in young rats with chronic cholestatic liver disease, Sci. Rep. 10 (2020) 7536.
[16] B. Lanz, V. Rackayova, O. Braissant, C. Cudalbu, MRS studies of neuroenergetics and glutamate/glutamine exchange in rats: extensions to hyperammonemic models, Anal. Biochem. 529 (2017) 245–269.
[17] O. Braissant, V.A. McLin, C. Cudalbu, Ammonia toxicity to the brain, J. Inherit. Metab. Dis. 36 (2013) 595–612.
[18] J. Mosso, T. Yin, C. Poitry-Yamate, D. Simicic, M. Lepore, V.A. McLin, O. Braissant, C. Cudalbu, B. Lanz, PET CMRglc mapping and (1)H-MRS show altered glucose uptake and neurometabolic profiles in BDL rats, Anal. Biochem. 647 (2022), 114606.
[19] E. Flatt, V.A. McLin, O. Braissant, K. Pierzchala, P. Mastromarino, S.O. Mitrea, D. Sessa, R. Gruetter, C. Cudalbu, Probiotics combined with rifaximin influence the neurometabolic changes in a rat model of type C HE, Sci. Rep. 11 (2021), 17988.
[20] V. Rackayova, E. Flatt, O. Braissant, J. Grosse, D. Capobianco, P. Mastromarino, M. McMillin, S. DeMorrow, V.A. McLin, C. Cudalbu, Probiotics improve the neurometabolic profile of rats with chronic cholestatic liver disease, Sci. Rep. 11 (2021) 2269.
[21] S.W. Brusilow, R.C. Koehler, R.J. Traystman, A.J. Cooper, Astrocyte glutamine synthetase: importance in hyperammonemic syndromes and potential target for therapy, Neurotherapeutics 7 (2010) 452–470.
[22] A. Rovira, B. Minguez, F.X. Aymerich, C. Jacas, E. Huerga, J. Cordoba, J. Alonso, Decreased white matter lesion volume and improved cognitive function after liver transplantation, Hepatology 46 (2007) 1485–1490.
[23] B. Minguez, A. Rovira, J. Alonso, J. Cordoba, Decrease in the volume of white matter lesions with improvement of hepatic encephalopathy, AJNR Am. J. Neuroradiol. 28 (2007) 1499–1500.
[24] A. Srivastava, S. Chaturvedi, R.K. Gupta, R. Malik, A. Mathias, N.R. Jagannathan, S. Jain, C.M. Pandey, S.K. Yachha, R.K.S. Rathore, Minimal hepatic encephalopathy in children with chronic liver disease: prevalence, pathogenesis and magnetic resonance-based diagnosis, J. Hepatol. 66 (2017) 528–536.
[25] M. Mendez, M. Mendez-Lopez, L. Lopez, A. Begega, M.A. Aller, J. Arias, J.L. Arias, Reversal learning impairment and alterations in the prefrontal cortex and the hippocampus in a model of portosystemic hepatic encephalopathy, Acta Neurol. Belg. 110 (2010) 246–254.
[26] M. Mendez, M. Mendez-Lopez, L. Lopez, M.A. Aller, J. Arias, J.L. Arias, Portosystemic hepatic encephalopathy model shows reversal learning impairment and dysfunction of neural activity in the prefrontal cortex and regions involved in motivated behavior, J. Clin. Neurosci. 18 (2011) 690–694.
[27] J. Alonso, J. Cordoba, A. Rovira, Brain magnetic resonance in hepatic encephalopathy, Semin. Ultrasound CT MR 35 (2014) 136–152.
[28] R. Datta, V. Sethi, S. Ly, A.T. Waldman, S. Narula, B.E. Dewey, P. Sati, D. Reich, B. Banwell, 7T MRI visualization of cortical lesions in adolescents and young adults with pediatric-onset multiple sclerosis, J. Neuroimaging 27 (2017) 447–452.

[29] J.P. Marques, T. Kober, G. Krueger, W. van der Zwaag, P.F. Van de Moortele, R. Gruetter, MP2RAGE, a self bias-field corrected sequence for improved segmentation and T1-mapping at high field, Neuroimage 49 (2010) 1271–1281.
[30] D. Schmitter, A. Roche, B. Marechal, D. Ribes, A. Abdulkadir, M. Bach-Cuadra, A. Daducci, C. Granziera, S. Kloppel, P. Maeder, R. Meuli, G. Krueger, I. Alzheimer's Disease Neuroimaging, An evaluation of volume-based morphometry for prediction of mild cognitive impairment and Alzheimer's disease, Neuroimage Clin. 7 (2015) 7–17.
[31] J. Boto, G. Gkinis, A. Roche, T. Kober, B. Marechal, N. Ortiz, K.O. Lovblad, F. Lazeyras, M.I. Vargas, Evaluating anorexia-related brain atrophy using MP2RAGE-based morphometry, Eur. Radiol. 27 (2017) 5064–5072.
[32] B. Morel, G.F. Piredda, J.P. Cottier, C. Tauber, C. Destrieux, T. Hilbert, D. Sirinelli, J.P. Thiran, B. Marechal, T. Kober, Normal volumetric and T1 relaxation time values at 1.5 T in segmented pediatric brain MRI using a MP2RAGE acquisition, Eur. Radiol. 31 (2021) 1505–1516.
[33] L. Xin, B. Schaller, V. Mlynarik, H. Lu, R. Gruetter, Proton T1 relaxation times of metabolites in human occipital white and gray matter at 7 T, Magn. Reson. Med. 69 (2013) 931–936.
[34] R. Mekle, V. Mlynarik, G. Gambarota, M. Hergt, G. Krueger, R. Gruetter, MR spectroscopy of the human brain with enhanced signal intensity at ultrashort echo times on a clinical platform at 3T and 7T, Magn. Reson. Med. 61 (2009) 1279–1285.
[35] S.W. Provencher, Automatic quantitation of localized in vivo 1H spectra with LCModel, NMR Biomed. 14 (2001) 260–264.
[36] V. Govindaraju, K. Young, A.A. Maudsley, Proton NMR chemical shifts and coupling constants for brain metabolites, NMR Biomed. 13 (2000) 129–153.
[37] V. Govind, K. Young, A.A. Maudsley, Corrigendum: proton NMR chemical shifts and coupling constants for brain metabolites. Govindaraju V, Young K, Maudsley AA, NMR Biomed. 2000; 13: 129-153, NMR Biomed. 28 (2015) 923–924.
[38] A. Lin, O. Andronesi, W. Bogner, I.Y. Choi, E. Coello, C. Cudalbu, C. Juchem, G. J. Kemp, R. Kreis, M. Krssak, P. Lee, A.A. Maudsley, M. Meyerspeer, V. Mlynarik, J. Near, G. Oz, A.L. Peek, N.A. Puts, E.M. Ratai, I. Tkac, P.G. Mullins, M.R.S. Experts' Working Group on Reporting Standards for, Minimum reporting standards for in vivo magnetic resonance spectroscopy (MRSinMRS): experts' consensus recommendations, NMR Biomed. 34 (2021) e4484.
[39] C. Juchem, C. Cudalbu, R.A. de Graaf, R. Gruetter, A. Henning, H.P. Hetherington, V.O. Boer, B(0) shimming for in vivo magnetic resonance spectroscopy: experts' consensus recommendations, NMR Biomed. 34 (2021), e4350.
[40] R. Garcia-Martinez, A. Rovira, J. Alonso, C. Jacas, M. Simon-Talero, L. Chavarria, V. Vargas, J. Cordoba, Hepatic encephalopathy is associated with posttransplant cognitive function and brain volume, Liver Transplant. 17 (2011) 38–46.
[41] A. Fitsiori, V. McLin, S. Toso, M.I. Vargas, Reversible brain atrophy after liver transplantation for biliary atresia in childhood, Neurol. Clin. Pract. 11 (2021) e923–e925.
[42] P. Moser, L. Hingerl, B. Strasser, M. Povazan, G. Hangel, O.C. Andronesi, A. van der Kouwe, S. Gruber, S. Trattnig, W. Bogner, Whole-slice mapping of GABA and GABA (+) at 7T via adiabatic MEGA-editing, real-time instability correction, and concentric circle readout, Neuroimage 184 (2019) 475–489.
[43] E.H. Baker, G. Basso, P.B. Barker, M.A. Smith, D. Bonekamp, A. Horska, Regional apparent metabolite concentrations in young adult brain measured by (1)H MR spectroscopy at 3 Tesla, J. Magn. Reson. Imag. 27 (2008) 489–499.
[44] M. Povazan, B. Strasser, G. Hangel, E. Heckova, S. Gruber, S. Trattnig, W. Bogner, Simultaneous mapping of metabolites and individual macromolecular components via ultra-short acquisition delay (1) H MRSI in the brain at 7T, Magn. Reson. Med. 79 (2018) 1231–1240.
[45] C. Cudalbu, K.L. Behar, P.K. Bhattacharyya, W. Bogner, T. Borbath, R.A. de Graaf, R. Gruetter, A. Henning, C. Juchem, R. Kreis, P. Lee, H. Lei, M. Marjanska, R. Mekle, S. Murali-Manohar, M. Povazan, V. Rackayova, D. Simicic, J. Slotboom, B.J. Soher, Z. Starcuk Jr., J. Starcukova, I. Tkac, S. Williams, M. Wilson, A. M. Wright, L. Xin, V. Mlynarik, Contribution of macromolecules to brain (1) H MR spectra: experts' consensus recommendations, NMR Biomed. 34 (2021), e4393.
[46] V.A. McLin, L. D'Antiga, The current pediatric perspective on type B and C hepatic encephalopathy, Anal. Biochem. 643 (2022), 114576.
[47] S. Gilmour, R. Adkins, G.A. Liddell, G. Jhangri, C.M. Robertson, Assessment of psychoeducational outcomes after pediatric liver transplant, Am. J. Transplant. 9 (2009) 294–300.
[48] C. Rose, R.F. Butterworth, J. Zayed, L. Normandin, K. Todd, A. Michalak, L. Spahr, P.M. Huet, G. Pomier-Layrargues, Manganese deposition in basal ganglia structures results from both portal-systemic shunting and liver dysfunction, Gastroenterology 117 (1999) 640–644.
[49] M.J. Versluis, W.M. Teeuwisse, H.E. Kan, M.A. van Buchem, A.G. Webb, M.J. van Osch, Subject tolerance of 7 T MRI examinations, J. Magn. Reson. Imag. 38 (2013) 722–725.
[50] D.K. Deelchand, P.G. Henry, J.M. Joers, E.J. Auerbach, Y.W. Park, F. Kara, E. M. Ratai, K. Kantarci, G. Oz, Plug-and-play advanced magnetic resonance spectroscopy, Magn. Reson. Med. 87 (2022) 2613–2620.
[51] G. Hangel, E. Niess, P. Lazen, P. Bednarik, W. Bogner, B. Strasser, Emerging methods and applications of ultra-high field MR spectroscopic imaging in the human brain, Anal. Biochem. 638 (2022), 114479.
[52] W. Bogner, R. Otazo, A. Henning, Accelerated MR spectroscopic imaging-a review of current and emerging techniques, NMR Biomed. 34 (2021), e4314.
[53] M. Wilson, O. Andronesi, P.B. Barker, R. Bartha, A. Bizzi, P.J. Bolan, K.M. Brindle, I.Y. Choi, C. Cudalbu, U. Dydak, U.E. Emir, R.G. Gonzalez, S. Gruber, R. Gruetter, R.K. Gupta, A. Heerschap, A. Henning, H.P. Hetherington, P.S. Huppi, R.E. Hurd, K. Kantarci, R.A. Kauppinen, D.W.J. Klomp, R. Kreis, M.J. Kruiskamp, M.O. Leach, A.P. Lin, P.R. Luijten, M. Marjanska, A.A. Maudsley, D.J. Meyerhoff, C. E. Mountford, P.G. Mullins, J.B. Murdoch, S.J. Nelson, R. Noeske, G. Oz, J.W. Pan, A.C. Peet, H. Poptani, S. Posse, E.M. Ratai, N. Salibi, T.W.J. Scheenen, I.C.P. Smith, B.J. Soher, I. Tkac, D.B. Vigneron, F.A. Howe, Methodological consensus on clinical proton MRS of the brain: review and recommendations, Magn. Reson. Med. 82 (2019) 527–550.
[54] F. Pittau, M.O. Baud, J. Jorge, L. Xin, F. Grouiller, G.R. Iannotti, M. Seeck, F. Lazeyras, S. Vulliemoz, M.I. Vargas, MP2RAGE and susceptibility-weighted imaging in lesional epilepsy at 7T, J. Neuroimaging 28 (2018) 365–369.